Membrane Water Treatment, *Vol. 6, No. 2 (2015) 113-126*
DOI: http://dx.doi.org/10.12989/mwt.2015.6.2.113

Solid-salt pressure-retarded osmosis with exothermic dissolution energy for sustainable electricity production

Wook Choi [2,3], Harim Bae [1,4], Pravin G. Ingole [2], Hyung Keun Lee [2], Sung Jo Kwak [1], Nam Jo Jeong [1], Soon-Chul Park [1], Jong Hak Kim [3], Jonghwi Lee [4] and Chul Ho Park [*1]

[1] *Jeju Global Research Center (JGRC), Korea Institute of Energy Research (KIER), 200 Haemajihaean-ro, Gujwa-eup, Jeju Specific Self-Governing Province 695-971, South Korea*
[2] *Greenhouse Gas Research Center, Korea Institute of Energy Research (KIER), 71-2 Jang-dong, Yuseong-gu, Daejeon 305-343, South Korea*
[3] *Department of Chemical and Biomolecular Engineering, Yonsei University, 50 Yonsei-Ro, Seondaemun-Gu, Seoul 120-749 South Korea*
[4] *Department of Chemical Engineering and Materials Science, Chung-Ang University, 221 Heukseok-Dong, Dongjak-gu, Seoul 156-756, South Korea*

(*Received October 01, 2014, Revised December 09, 2014, Accepted December 30, 2014*)

Abstract. Salinity gradient power (SGP) systems have strong potential to generate sustainable clean electricity for 24 hours. Here, we introduce a solid-salt pressure-retarded osmosis (PRO) system using crystal salt powders rather than seawater. Solid salts have advantages such as a small storage volume, controllable solubility, high Gibbs dissolution energy, and a single type of water intake, low pretreatment costs. The power densities with 3 M draw solutions were 11 W/m^2 with exothermic energy and 8.9 W/m^2 without at 35 bar using a HTI FO membrane (water permeability A = 0.375 L m^{-2} h^{-1} bar^{-1}). These empirical power densities are ~13% of the theoretical value.

Keywords: salinity gradient power; pressure-retarded osmosis; exothermic; calcium chloride; solid salt

1. Introduction

Electricity is the fundamental energy source for civilized and industrial society. With increasing in industrialization, the total energy consumption has increased by ~6% annually in global, supplied by more than 100 MW-sized power plants using hydroelectric, nuclear, and thermoelectric power (Vacancies 2012). However, these technologies are associated with environmental issues such as CO_2 emissions and therefore climate change. Accordingly, many countries have been developing and exploring various clean renewable energy technologies, e.g., photovoltaic, solar heat, wind, and ocean thermal energy conversion. Electricity must be supplied continuously to avoid blackouts under forecast loads. Therefore, it might be difficult for current renewable energies to dominantly serve as the primary electricity supply due to limitations in

*Corresponding author, Ph.D. Chul Ho Park, E-mail: chpark@kier.re.kr

Copyright © 2015 Techno-Press, Ltd.
http://www.techno-press.org/?journal=mwt&subpage=7 ISSN: 2005-8624 (Print), 2092-7037 (Online)

operating times.

Salinity gradient power (SGP) systems are a sustainable and renewable energy source candidate if two solutions with different salinities can be sustainably obtained. SGP was first proposed more than half a century ago (Pattle 1954). When seawater and river water are pumped into SGP systems near estuaries, the difference in osmotic pressure between the two solutions is about 24 bar (similar to 240 m hydroelectric potential). If the whole global river discharge volume is used for SGP, it could potentially produce the estimated 2 TW of electricity (Dai and Treberth 2002), 13% of global electricity consumption (La Mantia *et al*. 2011). Nevertheless, the development of SGP has been relatively slow despite great interest, due to insufficient progress in membrane science. In 2009, the world's first PRO power plant operated by Statkraft in Norway demonstrated the potential viability of SGP, but it might be economically infeasible due to low power density with low membrane performance.

SGP is based on extraction of Gibb's free energy generated by mixing a saline solution (e.g., seawater) and a freshwater solution (e.g., river water). The driving force is the difference in chemical potential of the solvent water between the two different concentration solutions separated by a membrane ($\Delta\mu$). At equilibrium, the chemical potential of the pure solvent (μ_w) can be expressed as follows

$$\mu_w^* = \mu_w(x_w, \pi - P) \tag{1}$$

where x_w is the mole fraction of the solvent (water molecules), P is the pressure (bar), and π is the osmotic pressure. PRO is a system for directly harvesting the osmotic pressure across a semi-permeable membrane with hydraulic pressure applied to a draw solution. The osmotic pressure (π) can be estimated using Van't Hoff equation as follows

$$\pi = iCRT \tag{2}$$

where C (mol/L) and T (K) are the concentration and temperature, R (8.3124 J/mol K) is the universal gas constant, and i is a Van't Hoff factor associated with the dissociation number of a solute. Based on the thermodynamic theory, Elimelech et al. calculated the highest extractable work for a constant-pressure PRO with a seawater draw solution (typically 600 mM) and a river water feed solution (1.5 mM), which was 0.75 kWh/m^3 with a free energy of mixing of 0.81 kWh/m^3 (Yip and Elimelech 2012).

With respect to economic feasibility, the membrane has constant water flux to maintain the sustainable power (Raluy *et al*. 2006). In natural surface waters, there are various contaminants that induce complex fouling phenomena. At a higher water flux, fouling is promoted by greater hydrodynamic force. Quanhong et al. systematically investigated organic fouling behaviors in PRO mode (She *et al*. 2013). Membranes in PRO mode (active layer facing the draw solution) typically generate higher water flux at the same osmotic pressure than membranes in forward osmosis (FO) mode (active layer facing the feed solution) due to lower internal concentration polarization (ICP). However, PRO mode is prone to fluting and has a less stable flux. The porous support layer of a membrane in PRO mode often gets clogged by foulants in feed river water. Another challenge is biofouling, which often occurs in both the feed and draw solutions when natural water sources are directly pumped into membrane modules without filtration. Typical natural water contains organic matter and microalgae that can foul the membrane surface, leading to loss of performance of the membrane (Paper 2011).

The pretreatment equipment used for seawater reverse osmosis (SWRO) facilities is similar to

that of drinking water treatment facilities. For example, flocculation and sedimentation are used to remove suspended materials and dissolved air flotation is used to remove algal biomass and hydrocarbons. Low-pressure ultrafiltration (UF) or microfiltration (MF) is used to remove suspended particulates. For surface water that requires extensive pretreatment, the energy consumption can be comparable to SWRO pretreatment, e.g., up to 0.05 kWh/m^3 for gravity granular filtration pretreatment and 0.2~0.4 kWh/m^3 for MF/UF membrane pretreatment (Voutchkov 2006). The energy consumption for pretreatment in a PRO system would likely be higher than that of SWRO due to the river and seawater intakes. If both water sources are filtered using MF/UF, the energy consumption would be around 0.4~0.8 kWh/m^3. As noted above, the theoretically extractable power of PRO is ~0.81 kWh/m^3. In addition, the energy required to pump the seawater must be considered (the pumping energy for the river water is negligible due to spontaneous water diffusion). Therefore, the energy consumption for pretreatment must be minimized to maximize the net energy efficiency of a PRO plant (Mi and Elimelech 2008).

Recently, several alternatives have been evaluated to enhance PRO power density without pretreatment. For example, the brine could be used in place of natural seawater. According to the Van't Hoff equation, a higher concentration saline solution produces higher power density. The Megaton Water System was developed in Japan in 2010 using the brine discharged from a SWRO system and in 2011, achieved a power density of 7.7 W/m^2 (Tanioka *et al*. 2012). In addition, a government-funded project (GMVP) in South Korea was launched in 2013 based on a SWRO-PRO-MD system to reduce the specific energy consumption of desalinization up to 1.6 kWh/m^3. Both projects suggest that pretreated clean brine has the potential to generate greater net power than that of natural seawater (Logan and Elimelech 2012). Furthermore, the optimization of hybrid desalinization with SGP using chemical potential energy may be more efficient than typical mechanical energy recovery systems (e.g., pressure exchangers), as well as more eco-friendly by diluting the brine concentration (Feinberg *et al*. 2013). If SWRO brine was not available, Elimelech et al. suggested an ammonia–carbon dioxide heat engine of 240 W/m^2 calculated by a theoretical function (Logan and Elimelech 2012, McGinnis *et al*. 2007). The concept shows that a low-grade heating system combined with a PRO system could be economically viable (Loeb 1975, McGinnis and Elimelech 2008).

As discussed above, present seawater/river water PRO systems may be uneconomical to positively generate electricity (of course, it would be dependent on intake qualities). However, PRO-optimized membranes and energy-efficient processes are approaching commercialization (Chou *et al*. 2012, Han *et al*. 2013, Ingole *et al*. 2014, Sun and Chung 2013, Yip *et al*. 2011). The goal of this study is to demonstrate a new strategy for expanding a SGP target market. We used solid salt powders as an energy source to induce a salinity gradient. The solid-salt system has several advantages: (1) the system does not require a large storage footprint, (2) the osmotic pressure is easily controllable, (3) a single type and source of water is required, reducing pretreatment costs, and (4) the brackish could be recycled by combining membrane distillation crystallization (Tun *et al*. 2005). Furthermore, because the solid salt releases Gibbs free energy during dissolution in pumped water, the osmotic pressure can be increased to greater than that solely.

2. Experimental

To construct the solid-salt PRO system, a HTI-ES flat-sheet semipermeable membrane was purchased from Hydration Technology Innovations LLC (USA) and a reverse osmosis module was

purchased from GE Water & Process Technologies (USA; membrane area, 133 cm^2). The flow volumes of the draw and feed solutions were controlled using HPLC pumps (Series II; Scientific Systems Inc., USA). The flow rates of the draw and feed solutions were 7 and 14 mL/min, respectively, which were optimized and set to the highest water flux using polypropylene woven screen-mesh spacers (the mesh sizes of the draw and feed sides were 50 and 300 μm, respectively, to reduce external concentration polarization). A backpressure regulator (Parker, USA) was installed to pressurize the draw solution passing through the active surface side of the membrane module. The active layer of the membrane was always facing the draw solution. The draw solutions were prepared to 0.6~6.8 M using $CaCl_2$ (dehydrate grade 99%; Samchun Pure Chemical

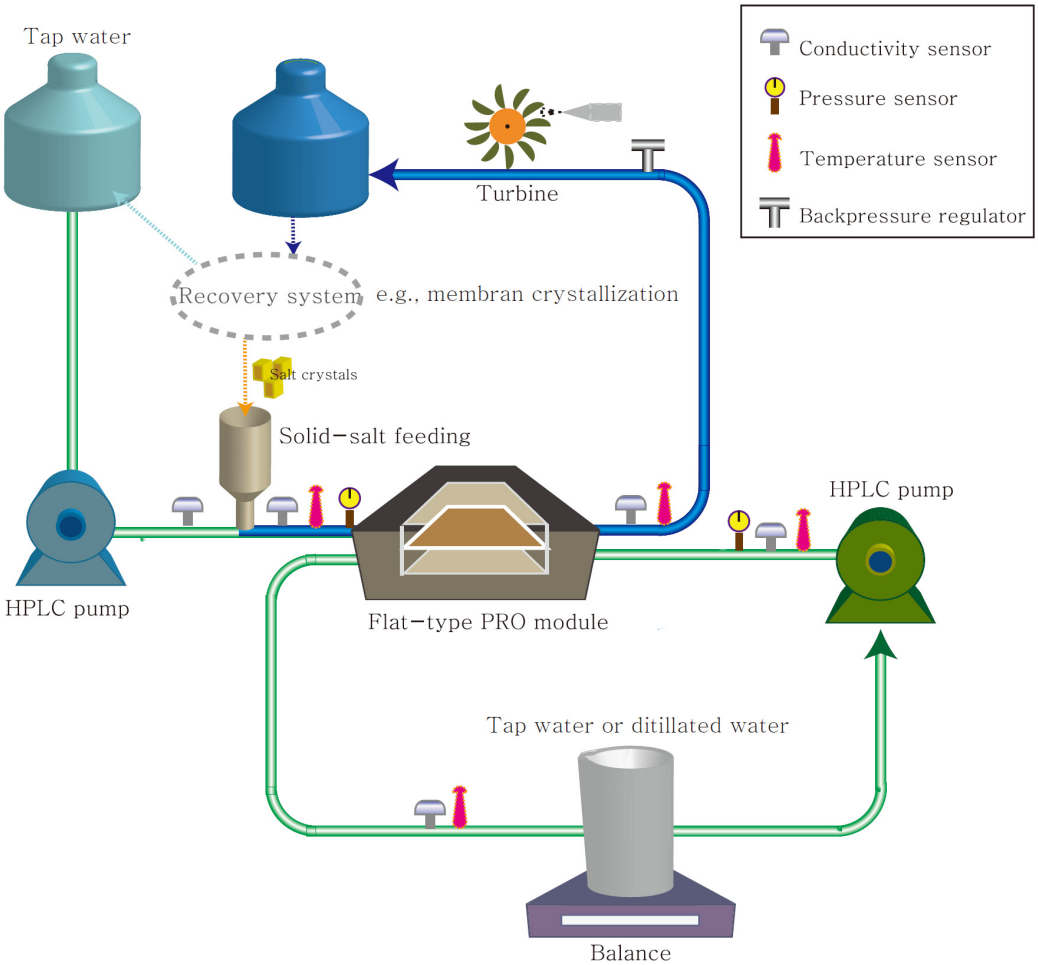

Fig. 1 Schematic representation of a solid-salt PRO system. For the lab-scale PRO test, the permeable water flux was measured by an electronic balance. The pressure, conductivity, and temperature were measured at the inlet/outlet points. The pressure on the draw side was controlled by a backpressure regulator. For an independent power system, the solid salt would be fed into the feed pipeline. A Pelton turbine would be recommended for power generation, because the nozzle could be controlled and pressurized by a signal from the conductivity sensor at the inlet for the draw solution

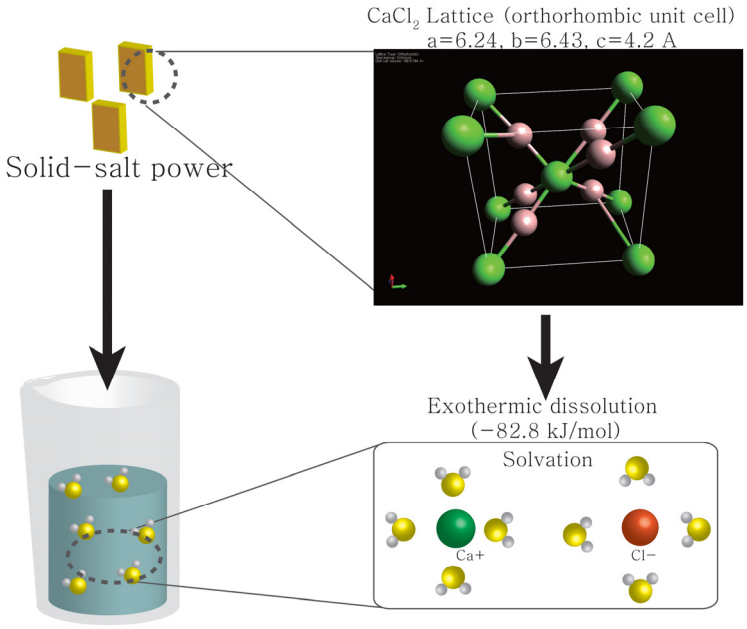

Fig. 2 Schematic representation of exothermic dissolution of $CaCl_2$ crystal powders. During solvation, the lattice energy becomes exothermic heat energy. Negative symbols indicate an exothermic process

Co., South Korea) with tap water (260 μS/cm at 20°C). Tap water was used for the feed solution because it would be an available water source for an independent power system. To minimize heat loss from the pump head, module, and tube, a bench-scale PRO system was isolated in a temperate-controlled chamber constructed for the study. A general schematic of the flow process for a solid-salt system is shown in Fig. 1. The concentration of the draw solution can be controlled by changing the feeding relative velocity of both the tap water and the salt powders. Electricity can be provided by a Pelton turbine, because of the low flow rate and high pressure. On demand, a desalinization system could be incorporated to recycle the brackish water. There are several options, but the study recommends membrane distillation crystallization with waste-heat of solar-heat to reduce the energy consumption (Cipollina *et al*. 2012, Tun *et al*. 2005, Yun *et al*. 2006). In this study, the power density was calculated using the permeate flux and applied pressure.

The membrane permeate flux, J_w (i.e., the volumetric flux of water), was determined by measuring the change in the weight of the feed tank using an electronic balance (Mettler-Toledo, USA) every 5 min. The water flux J_w (m s^{-1}) across the membrane is given by

$$J_w = A(\Delta\pi_m - \Delta P) \tag{3}$$

where A is the intrinsic water permeability coefficient (L m^{-2} h^{-1} bar^{-1}) of the membrane, $\Delta\pi_m$ is the effective osmotic pressure across the active layer, and ΔP is the applied hydraulic pressure difference across the membrane. The water permeability coefficient, A, is calculated by dividing the distilled water flux (15 μS/cm at 20°C) by the applied pressure in RO mode (Yip *et al*. 2011)

$$A = \frac{J_w^{DI}}{\Delta P} \tag{4}$$

3. Results and discussion

A solid-salt PRO system such as the one tested here is relatively free from geographical constraints because of the availability of water nearly anywhere. However, solid salts as the fundamental energy source must be supplied to ensure a stable supply of electricity. Many clean and safe salts could become a candidate for solid-salt PRO systems. In particular, draw materials developed for forward osmosis systems could be also used (Cath *et al*. 2006). After screening several hundred inorganic salts, $CaCl_2$ was selected as a model material. It is a widely used salt in winter for snow removal, because it has very low toxicity and is not harmful to humans. Another important criterion is the price of ~$100/ton, as high-quality crystals are not required for solid-salt systems. With respect to physicochemical properties, it has high solubility and high exothermic dissolution energy. The crystal structure of its anhydride forms is orthorhombic with lattice parameters of a = 6.24, b = 6.43, and c = 4.2 (Fig. 3) (Radhakrishnan and Saini 1993). The dissolution of $CaCl_2$ in water is an exothermic reaction that releases ~82.8 kJ/mol. Therefore, it is a good candidate for evaluating the merits of solid-salt PRO systems with spontaneous exothermic energy.

If the system is perfectly isolated, the exothermic energy could become an additional source to spontaneously increase the solution temperature in a concentration-dependent manner (Fig. 3(a)). In an actual system, the solid-salt powder would be fed into a pipeline in front of the entrance of the draw side of the PRO module. Because $CaCl_2$ readily dissolves in water, the length of the pipeline to the module can be reduced and thermal energy conserved. The expected osmotic pressure can be calculated using the Van't Hoff equation (Fig. 3(b)). At low concentrations (e.g.,

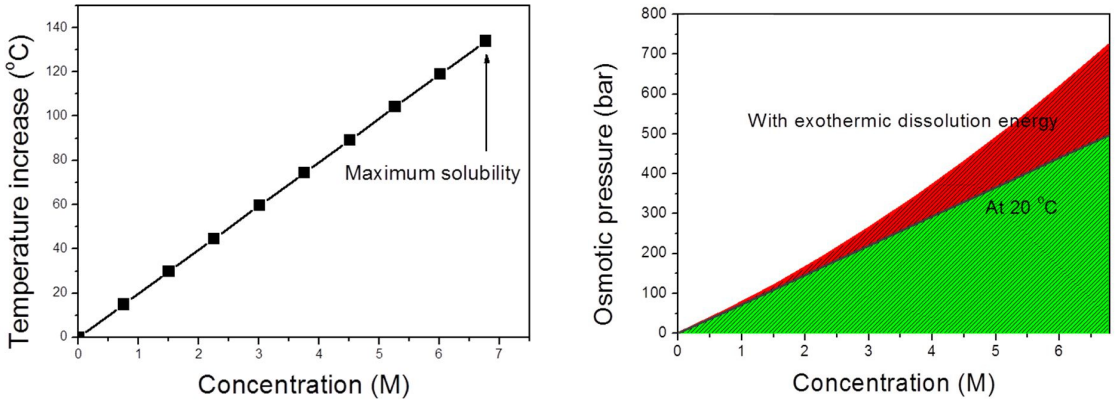

(a) (b)

Fig. 3 (a) Temperature increase as a function of concentration. At saturation, the temperature has increased by 135°C; (b) osmotic pressure difference with and without exothermic energy. Without a change in temperature (e.g., at 20 °C), the osmotic pressure is linearly proportional to the concentration of $CaCl_2$

1 M), the exothermic effect is imperceptible. However, at the saturation concentration (6.8 M), the temperature of the solution greatly increases by up to 135°C. This increase in temperature spontaneously raises the osmotic pressure to 723 bar when the temperature of the feeding solution is ~20°C. Cath *et al*. (2006) also calculated the osmotic pressure as a function of the concentration of $CaCl_2$ using a chemical simulation program (OLI Stream Analyzer) (Cath *et al*. 2006). Interestingly, their osmotic pressure values are higher than our calculated values, e.g., ~1000 bar at 5 M $CaCl_2$. While the exact relationship between concentration and osmotic pressure is uncertain, it is clear that the exothermic effect substantially increases the osmotic pressure.

The driving force is the difference in osmotic pressure across the membrane. The water permeation changes with continuous penetration of water molecules along the membrane surface in the module at a given flow rate (typically a linear velocity of 0.25 m/s is recommended to achieve the water permeability coefficient but in this study, the flow rate lower than 0.25 m/s for optimization of exothermic dissolution energy design) (Cath *et al*. 2013). Dilution consequently occurs and leads to a decline in osmotic pressure. Consider an initial draw solution concentration of $C_{D,0}$ and a volume flow rate of $Q_{D,0}$ as illustrated in Fig. 4. The draw solution concentration $C_{D,z}$

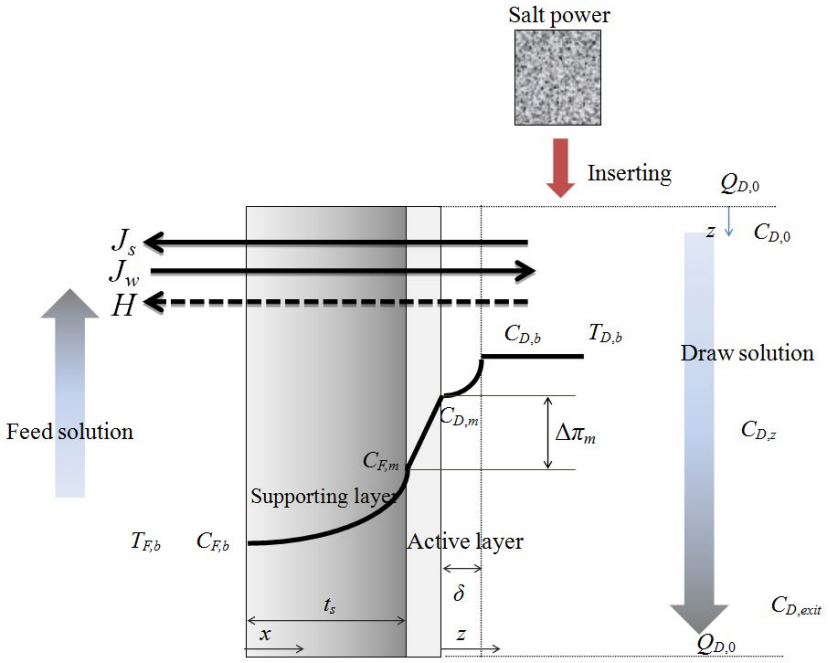

Fig. 4 Schematic representation of the salt concentration profile across a thin-film composite membrane in PRO mode at steady-state. The feed and draw solutions are introduced to the membrane in counter-flow. Dilutive external concentration polarization occurs in the mass transfer boundary layer of the draw solution, reducing the local concentration in the active layer from $C_{D,b}$ to $C_{D,m}$. Concentrative internal concentration polarization takes place within the porous supporting layer, increasing the local concentration at the active-support interface from $C_{F,b}$ to $C_{F,m}$. Concentrative external concentration polarization in the feed solution is assumed to be negligible. The pressurized draw solution creates a hydraulic pressure drop across the membrane, ΔP, which is lower than the osmotic pressure difference across the membrane

at certain points inside the module can be estimated as follows

$$C_{D,z} = C_{D,0}\left\{\frac{Q_{D,o}}{Q_{D,o} + \int_o^z J_w dA_m}\right\} \tag{5}$$

where A_m is the membrane area and the term $\int_o^z J_w dA_m$ corresponds to the cumulative permeated volume from the initial location to position z. Thus, $C_{D,z}$ is calculated using $C_{D,0}$ and the volumetric dilution factor $\left(\frac{Q_{D,o}}{Q_{D,o} + \int_o^z J_w dA_m}\right)$ and the diluted concentration of the draw solution $C_{D,exit}$ is obtained as follows

$$C_{D,exit} = C_{D,0}\left\{\frac{Q_{D,o}}{Q_{D,o} + Q_p}\right\} \tag{6}$$

where Q_p is the total permeated volume in the entire membrane module, i.e.,

$$Q_p = \int_0^{exit} J_w dA_m \tag{7}$$

The average flux $\bar{J}_w$ (m/s) in the module is given by

$$\bar{J}_w = \frac{Q_p}{A_m} \tag{8}$$

The average water flux is typically lower than the calculated value because in actual systems, there is both internal and external concentration polarization and reverse flux of salts on or within the membrane interface (Achilli *et al*. 2009). The practical flux is a function of membrane parameters (i.e., the support layer structural parameter *S*, the active layer salt permeability *B*, and the active layer water permeability *A*). For thin-film polyamide active layer membranes commercially available for reverse osmosis systems, *S* values are ~10,000 μm due to the operating pressure (i.e., > 50 bar); however, the *S* for PRO systems should be < 1000 μm (Elimelech *et al*. suggests an *S* value of 100 μm for high-performance PRO systems with seawater and river water intakes) (Yip and Elimelech 2011). Currently, there are no commercially available PRO membranes. Accordingly, the development of effective PRO membranes to enhance the maximum power density is an area of active current research.

Although the extractable power using the available membranes is currently limited, the theoretical maximum power density can be calculated by measuring the average water flux. The power density, i.e., the total power normalized by the membrane area in the module, is given by

$$W = \Delta P \times \bar{J}_w \tag{9}$$

Eq. (9) gives the power density of $CaCl_2$ systems with or without exothermic dissolution

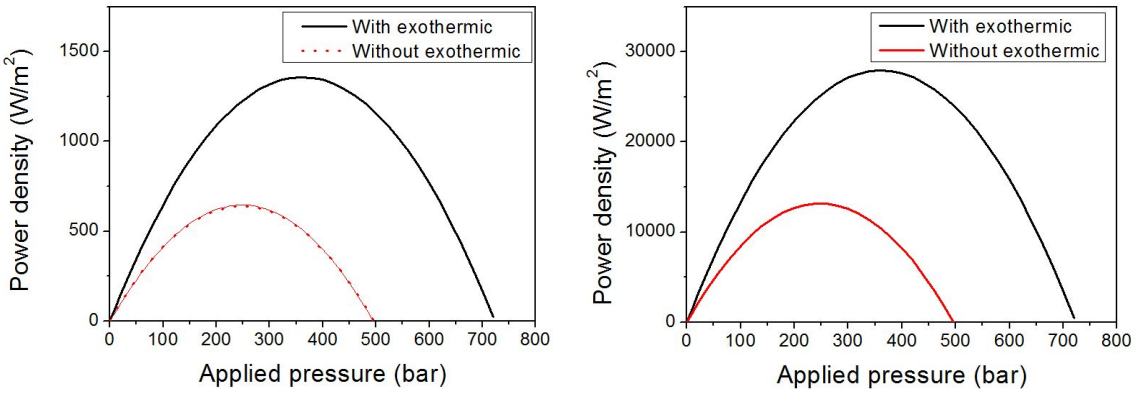

Fig. 5 Power density of $CaCl_2$ at saturation (6.7 M) with and without the exothermic dissolution energy using the permeability coefficient A for (a) HTI-FS membranes of 0.375 L m^{-2} h^{-1} bar^{-1}; or (b) thin-film polyamide membranes of 7.7 L m^{-2} h^{-1} bar^{-1}

energy. As noted above, the average water flux is greatly dependent on the water permeability coefficient A of the membrane. In this study, a cellulose triacetate FO membrane (HTI-ES flat membrane) was used with a water permeability coefficient of 0.375 L m^{-2} h^{-1} bar^{-1}. The maximum theoretical power density ($W_{max} = A \times \pi^2 / 4$) is about 638 W/m^2 at 247 bar without exothermic energy and 1360 W/m^2 at 360 bar with exothermic energy. These values represent the highest power density for a PRO system reported to date, despite the low permeability coefficient.

Furthermore, if thin-film polyamide active layer membranes (A = 7.7 L m^{-2} h^{-1} bar^{-1}) (Helfer *et al*. 2014) were introduced into the exothermic PRO system, the maximum power density could reach 28 kW/m^2 with exothermic dissolution energy (Fig. 5). These data suggest that a 1-m^2 membrane may be sufficient to construct a 28 kW power plant with low capital and membrane costs. Therefore, for solid-salt PRO systems, the exothermic energy is an important energy source, allowing production of twice the energy at the same saturation concentration (6.8 M).

There are clearly important limitations with respect to the mechanical strength of the membrane in an actual plant. SWRO type membranes are designed for structural support under an applied pressure of 60 bar (Lee *et al*. 2011). The mechanical strength is directly dependent on the structure parameters (S value) of the supporting layer (e.g., thickness, porosity, and tortuosity). Therefore, it would be difficult to enhance both physical properties due to typically trade-off relationship. One recently reported approach had provided a solution how to increase operating pressures without changing any structure parameters; thus, use of a flat module that could accommodate applied pressure of up to 48 bar with a power density of 60 W/m^2 using a thin-film composite membrane 200 μm in thickness (Straub *et al*. 2013). Therefore, design of solid-salt modules might be significant to generate high power.

In an SGP system, the water flux through the membrane increases with increasing osmotic pressure differential. However, there is always some deviation in the empirical results from the theoretical values. For example, a 5-fold difference in osmotic pressure increased the water flux by 3-fold in one reported experiment (Helfer *et al*. 2014). This non-linear relationship takes place due to concentration polarization. If deionized water is used as the feed solution, internal concentration polarization may be negligible when high salt rejection membranes are used. However, reduced

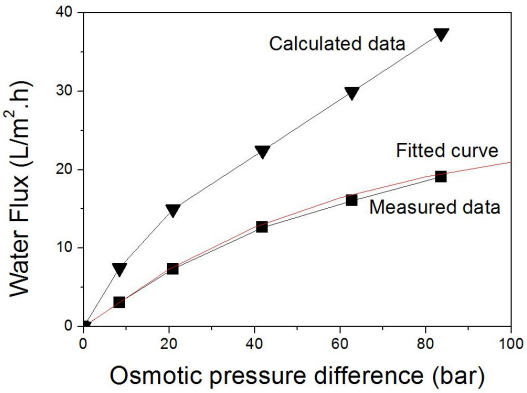

Fig. 6 Water flux as a function of the osmotic pressure difference (with a feed solution in distilled water). The water flux from a fitted curve has an empirical function ($25.6 - 25.7 \times 0.98^{\text{osmotic pressure}}$), meaning that the deviation between measured and calculated water flux increases with increasing the osmotic pressure

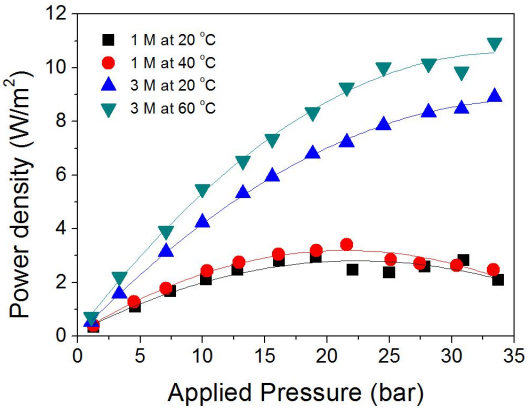

Fig. 7 Power density as a function of the applied hydraulic pressure for various concentrations of $CaCl_2$ and temperatures

power density can occur due to external concentration polarization during dilution of the draw solution at the membrane surface. When we measured the concentration (osmotic pressure) effect on the water flux at a linear flow rate under turbulent conditions, the water flux did not follow the relationship in Eq. (3). We tested $CaCl_2$ at the osmotic pressure difference as a function of concentration and the water flux followed the fitted curve in Fig. 6. Apparently, our module was not optimized to minimize external concentration polarization and the measured water flux waslower than the calculated flux. The deviation increased with increasing osmotic pressure difference due to insufficient dilution on the draw side. Future improvements in the design of the module are expected to enhance the water flux.

The relationship between the osmotic pressure and solution temperature is shown in Fig. 3(a). The temperature increase due to exothermic energy is dependent on the concentration. At 1 M $CaCl_2$, the temperature of the draw solution increased by 40°C. To evaluate the exothermic effect, the PRO module was placed in a chamber held at the same temperature. As shown in Fig. 7, 1 M

$CaCl_2$ produced only a slight increase in power density, although the osmotic pressure increased. The inlet temperature of the tap water was ~20°C, while the outlet temperature of the draw solution was ~30°C. Thus, heat exchange occurred within the module. With 3 M $CaCl_2$, the temperature of the draw solution increased by 60°C, sufficient to exhibit an exothermic effect. At 35 bar, the power density increased by ~20%. In this experiment, cellulose triacetate FO membranes were used. If another type of membrane (i.e., polyamide FO membranes) were used, we expect that a power density could be obtained of > 4 times our current results (Straub *et al*. 2013). However, the module must be optimized to reduce heat exchange as well as external concentration polarization. In addition, there would be some internal concentration polarization due to use of tap water and salt permeation (the salt rejection of a HTI FO membrane was ~ 92% at higher applied pressure than 15 bar). Nevertheless, the results of this study suggest that exothermic salts could become a significant clean energy source, generating more power than a typical seawater–river water SGP system.

4. Conclusions

For use during emergencies, standby generators have been required to be incorporated into a variety of buildings as backup electrical systems. One of most widely used standby generators is a diesel generator, which provides electricity to the main circuit during power outages in hospitals and other buildings. However, many countries have been working to reduce the CO_2 emissions produced by diesel and other hydrocarbon fuel sources. The solid-salt PRO system could serve as an alternative clean energy source under these circumstances. Typical domestic homes in South Korea consume about 15 kWh/d. With development of advanced membranes, high power density can be achieved using this solid-salt PRO system (theoretically 28 kW/m^2). Using a 1-m^2 membrane module, a solid-salt PRO system could be used as a standby or independent power generator for an individual home. Unfortunately, under the available applied pressure (35 bar) and the concentration (3 M), the empirical data (11 W/m^2) with HTI-ES membranes does not show the efficient power density with exothermic energy, compared to theoretical values (84 W/m^2) due to limited functions of membranes and modules. However, because the recent development of PRO-specialized membranes to produce higher power density has bolstered expectations of cost-effective and realizable power production (Chou *et al*. 2012, Yip *et al*. 2011), solid-salt PRO systems could hold a great potential to open SGP markets in the future.

Acknowledgments

This work was conducted under the Research and Development Program of the Korea Institute of Energy Research (KIER) (B4-2451-01).

References

Achilli, A., Cath, T.Y. and Childress, A.E. (2009), "Power generation with pressure retarded osmosis: An experimental and theoretical investigation", *J. Membr. Sci*., **343**(1-2), 42-52.

Cath, T.Y., Childress, A.E. and Elimelech, M. (2006), "Forward osmosis: Principles, applications, and recent developments", *J. Membr. Sci*., **281**(1-2), 70-87.

Cath, T.Y., Elimelech, M., McCutcheon, J.R., McGinnis, R.L., Achilli, A., Anastasio, D., Brady, A.R., Childress, A.E., Farr, I.V., Hancock, N.T., Lampi, J., Nghiem, L.D., Xie, M. and Yip, N.Y. (2013), "Standard methodology for evaluating membrane performance in osmotically driven membrane processes", *Desalination*, **312**, 31-38.

Chou, S., Wang, R., Shi, L., She, Q., Tang, C. and Fane, A.G. (2012), "Thin-film composite hollow fiber membranes for pressure retarded osmosis (PRO) process with high power density", *J. Membr. Sci.*, **389**, 25-33.

Cipollina, A., Di Sparti, M.G., Tamburini, A. and Micale, G. (2012), "Development of a membrane distillation module for solar energy seawater desalination", *Chem. Eng. Res. Des.*, **90**(12), 2101-2121.

Dai, A. and Treberth, K.E. (2002), "Estimates of freshwater dicharge from continents: Lattudial and seasonal variations", *J. Hydrometeorol.*, **3**(6), 660-687.

Feinberg, B.J., Ramon, G.Z. and Hoek, E.M.V. (2013), "Thermodynamic analysis of osmotic energy ecovery at a reverse osmosis desalination plant", *Environ. Sci. Technol.*, **47**(6), 2982-2989.

Han, G., Wang, P. and Chung, T.-S. (2013), "Highly robust thin-film composite pressure retarded osmosis (PRO) hollow fiber membranes with high power densities for renewable salinity-gradient energy generation", *Environ. Sci. Technol.*, **47**(14), 8070-8077.

Helfer, F., Lemckert, C. and Anissimov, Y.G. (2014), "Osmotic power with pressure retarded osmosis: Theory, performance and trends – A review", *J. Membr. Sci.*, **453**, 337-358.

Ingole, P.G., Choi, W., Kim, K.H., Park, C.H., Choi, W.K. and Lee, H.K. (2014), "Synthesis, characterization and surface modification of PES hollow fiber membrane support with polydopamine and thin film composite for energy generation", *Chem. Eng. J.*, **243**, 137-146.

La Mantia, F., Pasta, M., Deshazer, H.D., Logan, B.E. and Cui, Y. (2011), "Batteries for efficient energy extraction from a water salinity difference", *Nano Lett.*, **11**(4), 1810-1813.

Lee, K.P., Arnot, T.C. and Mattia, D. (2011), "A review of reverse osmosis membrane materials for desalination − Dvelopment to date and future potential", *J. Membr. Sci.*, **370**(1-2), 1-22.

Loeb, S. (1975), "Method and apparatus for generating power utilizing pressure-retarded-osmosis", Google Patents.

Logan, B.E. and Elimelech, M. (2012), "Membrane-based processes for sustainable power generation using water", *Nature*, **488**(7411), 313-319.

McGinnis, R.L. and Elimelech, M. (2008), "Global challenges in energy and water supply: The promise of engineered osmosis", *Environ. Sci. Technol.*, **42**(23), 8625-8629.

McGinnis, R.L., McCutcheon, J.R. and Elimelech, M. (2007), "A novel ammonia-carbon dioxide osmotic heat engine for power generation", *J. Membr. Sci.*, **305**(1-2), 13-19.

Mi, B. and Elimelech, M. (2008), "Chemical and physical aspects of organic fouling of forward osmosis membranes", *J. Membr. Sci.*, **320**(1-2), 292-302.

Paper, W. (2011), "Seawater desalination power consumption", *Water Reuse Association*, **11**(1~16).

Pattle, R. (1954), "Production of electric power by mixing fresh and salt water in the hydroelectric pile", *Nature*, **174**, 660 p.

Radhakrishnan, S. and Saini, D.R. (1993), "Polymer-induced crystallization of inorganic salts II. PEO-$CaCl_2$, PEO-K_2CO_3 and PEO-$CaCO_3$", *J. Crystal Growth*, **129**(1-2), 191-201.

Raluy, G., Serra, L. and Uche, J. (2006), "Life cycle assessment of MSF, MED and RO desalination technologies", *Energy*, **31**(13), 2361-2372.

She, Q., Wong, Y.K.W., Zhao, S. and Tang, C.Y. (2013), "Organic fouling in pressure retarded osmosis: Experiments, mechanisms and implications", *J. Membr. Sci.*, **428**, 181-189.

Straub, A.P., Yip, N.Y. and Elimelech, M. (2013), "Raising the bar: Increased hydraulic pressure allows unprecedented high power densities in pressure-retarded osmosis", *Environ. Sci. Technol. Lett.*, **1**(1), 55-59.

Sun, S.-P. and Chung, T.-S. (2013), "Outer-selective pressure-retarded osmosis hollow fiber membranes from vacuum-assisted interfacial polymerization for osmotic power generation", *Environ. Sci. Technol.*, **47**(22), 13167-13174.

Tanioka, A., Saito, K., Irie, M., Zaitsu, S., Sakai, H. and Hayashi, H. (2012), "Power generation by pressure

retarded osmosis using concentrated brine from seawater desalination system and treated sewage: Review of experience with pilot plant in Japan", *The 3rd Osmosis Membrane Summit*, 4, 1-33.

Tun, C.M., Fane, A.G., Matheickal, J.T. and Sheikholeslami, R. (2005), "Membrane distillation crystallization of concentrated salts-flux and crystal formation", *J. Membr. Sci.*, **257**(1-2), 144-155.

Vacancies, P.S. (2012), "Energy balances of non-OECD countries", *Int. Energy Agency*, 1-452.

Voutchkov, N. (2006), "Innovative method to evaluate tolerance of marine organism", *Desalin. Water Reuse*, **16**(2), 29-34.

Yip, N.Y. and Elimelech, M. (2011), "Performance limiting effects in power generation from salinity gradients by pressure retarded osmosis", *Environ. Sci. Technol.*, **45**(23), 10273-10282.

Yip, N.Y. and Elimelech, M. (2012), "Thermodynamic and energy efficiency analysis of power generation from natural salinity gradients by pressure retarded osmosis", *Environ. Sci. Technol.*, **46**(9), 5230-5239.

Yip, N.Y., Tiraferri, A., Phillip, W.A., Schiffman, J.D., Hoover, L.A., Kim, Y.C. and Elimelech, M. (2011), "Thin-film composite pressure retarded osmosis membranes for sustainable power generation from salinity gradients", *Environ. Sci. Technol.*, **45**(10), 4360-4369.

Yun, Y., Ma, R., Zhang, W., Fane, A.G. and Li, J. (2006), "Direct contact membrane distillation mechanism for high concentration NaCl solutions", *Desalination*, **188**(1-3), 251-262.

CC

Nomenclature

$\Delta\mu$	difference in chemical potential
μ_w	chemical potential of the pure solvent
x_w	mole fraction of the solvent
P	pressure (bar)
H	thermal diffusion (cal)
π	osmotic pressure (bar)
C	concentration of solution (M)
T	temperature (K)
R	universal gas constant (8.3124 J/mol K)
I	Van't Hoff factor
J_w	water flux (m s^{-1})
J_w^{DI}	water flux of distilled water in RO mode (m s^{-1})
$\bar{J}_w$	average water flux (m s^{-1})
A	water permeability coefficient (L m^{-2} h^{-1} bar^{-1})
$\Delta\pi_m$	effective osmotic pressure difference across the active layer (bar)
ΔP	hydraulic pressure difference (bar)
$C_{D,0}$	initial draw solution concentration (M)
$Q_{D,0}$	volume flow rate (m s^{-1})
$C_{D,z}$	draw solution concentration at certain points
A_m	membrane area (m^2)
$C_{D,exit}$	diluted concentration of the draw solution (M)
Q_p	total permeated volume (m^3)
W	power density (W/m^2)
$W_{\max}$	maximum power density (W/m^2)